

High proton conductivity in cyanide-bridged metal-organic frameworks: understanding the role of water

Yuan Gao, Richard Broersen, Wouter Hageman, Ning Yan, Marjo C. Mittelmeijer-Hazeleger, Gadi Rothenberg, Stefania Tanase*

Van 't Hoff Institute for Molecular Sciences, University of Amsterdam, Science Park 904, 1098XH Amsterdam, The Netherlands

Electronic Supporting Information

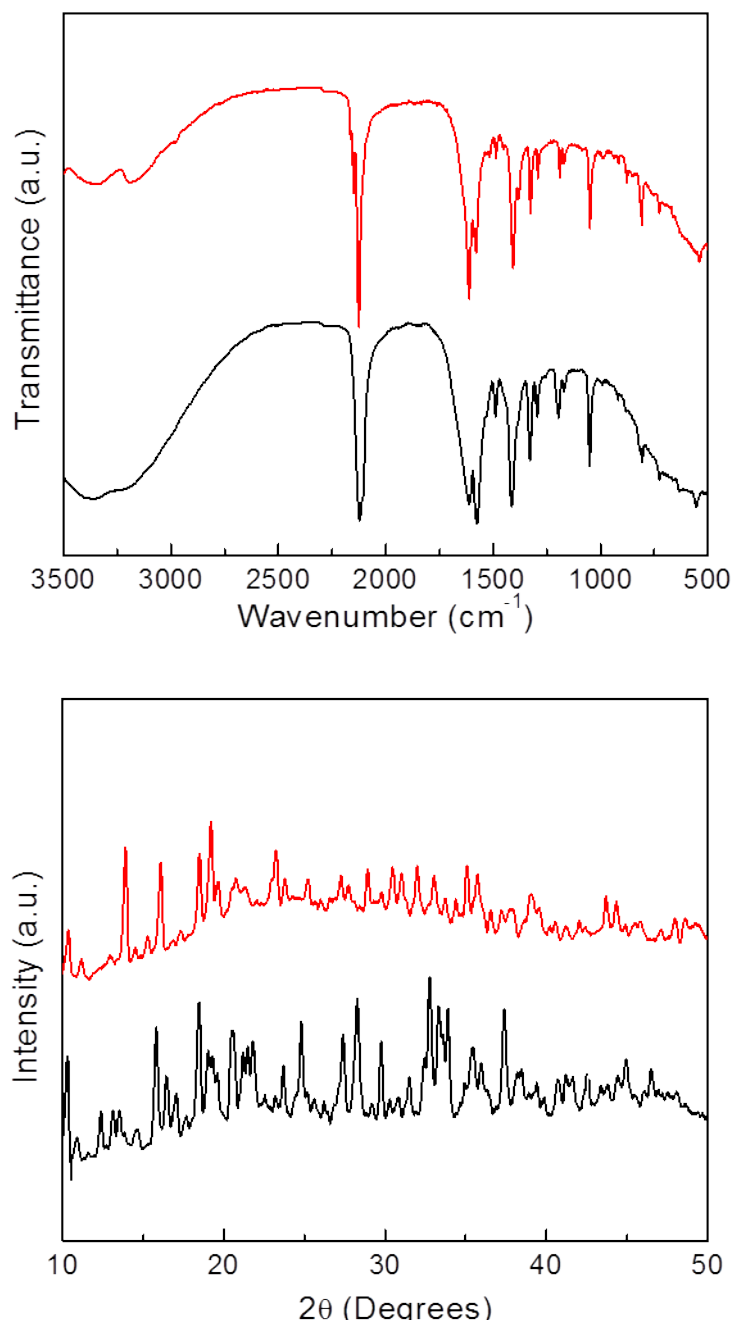


Figure S1. IR spectra (top) and PXRD patterns (bottom) for the as-synthesised NdMo-MOF (black), and for the NdMo-MOF activated at 80 °C (red).

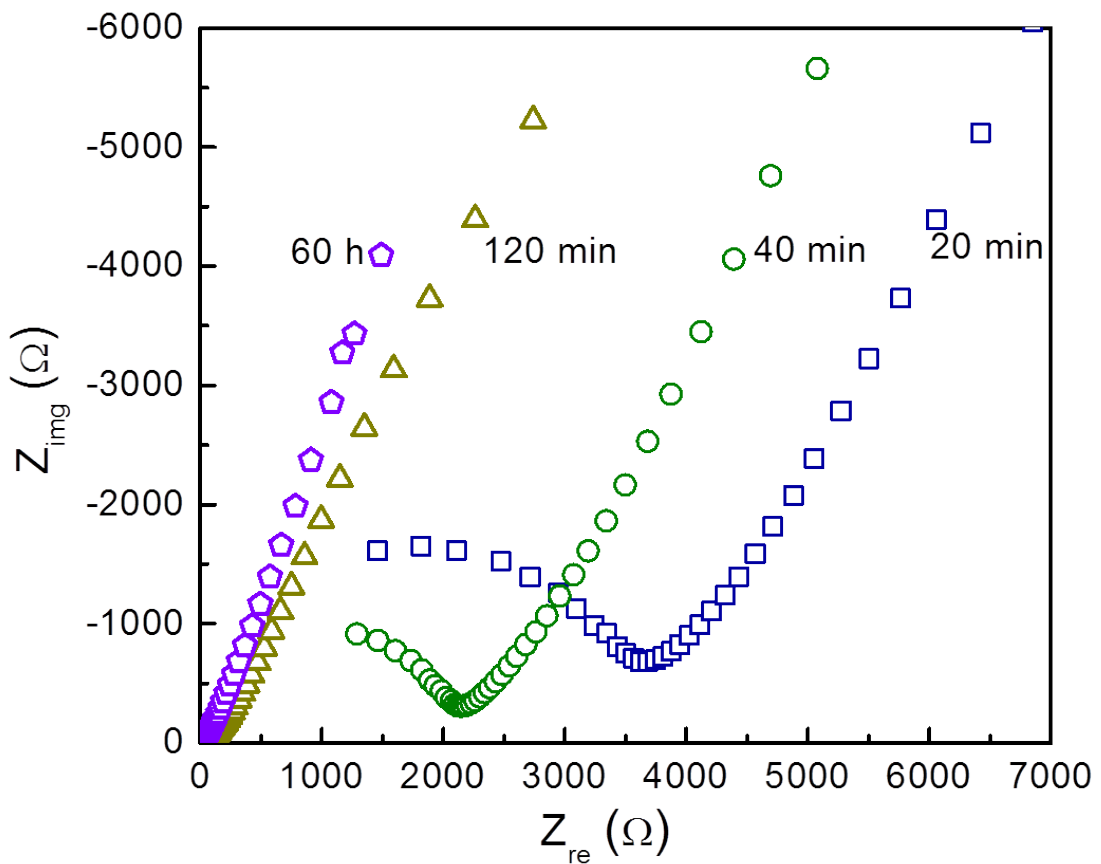


Figure S2. Influence of the equilibrium time on the proton conductivity measured at 21 °C and 26% RH for the NdMo-MOF activated at 80 °C.

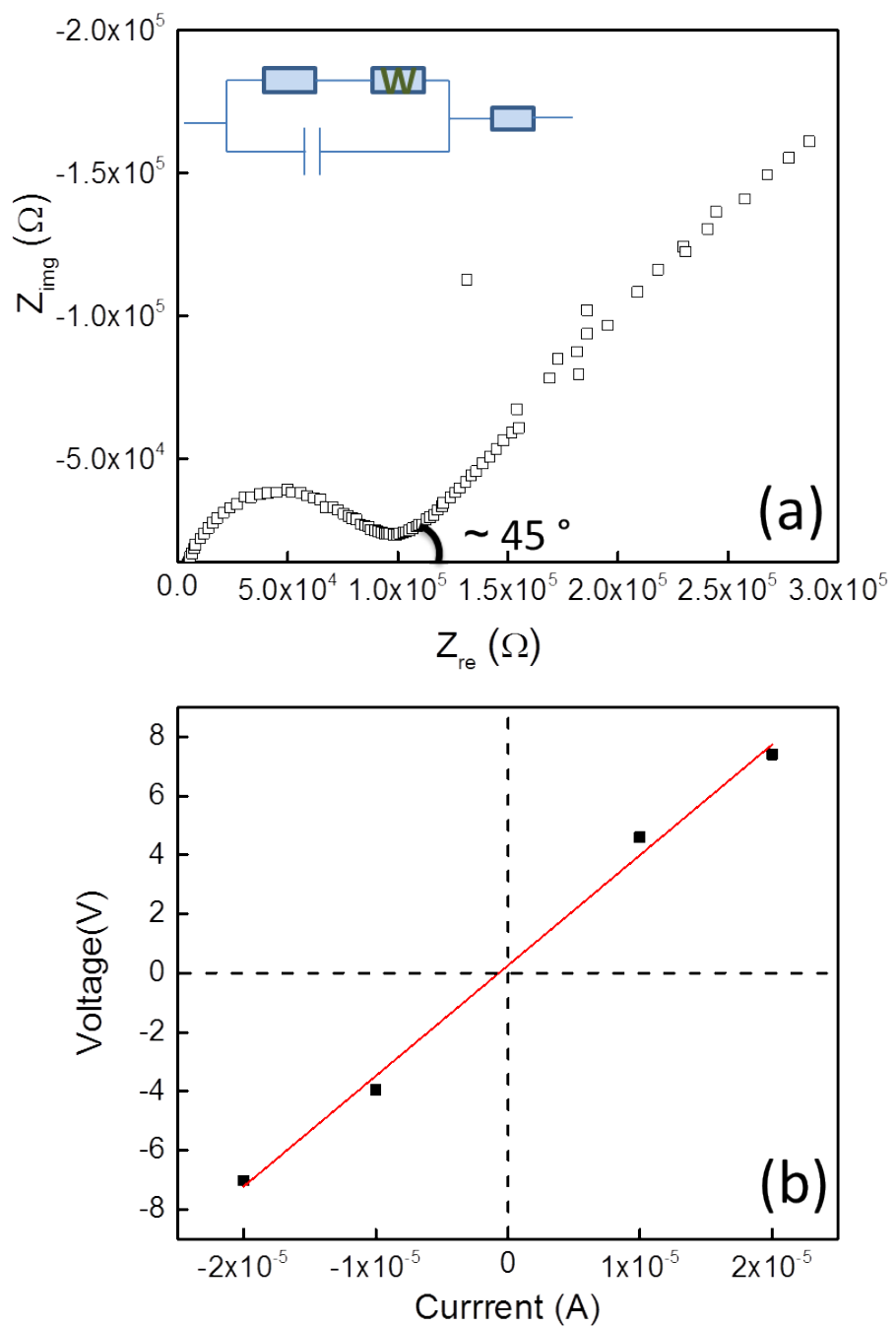


Figure S3. (a) Standard Nyquist plots for the as-synthesised NdMo-MOF measured at 21 °C and 26% RH. The inset shows the Warburg equivalent circuit. (b) DC conductivity measured at 21 °C and 26% RH for the as-synthesised NdMo-MOF.

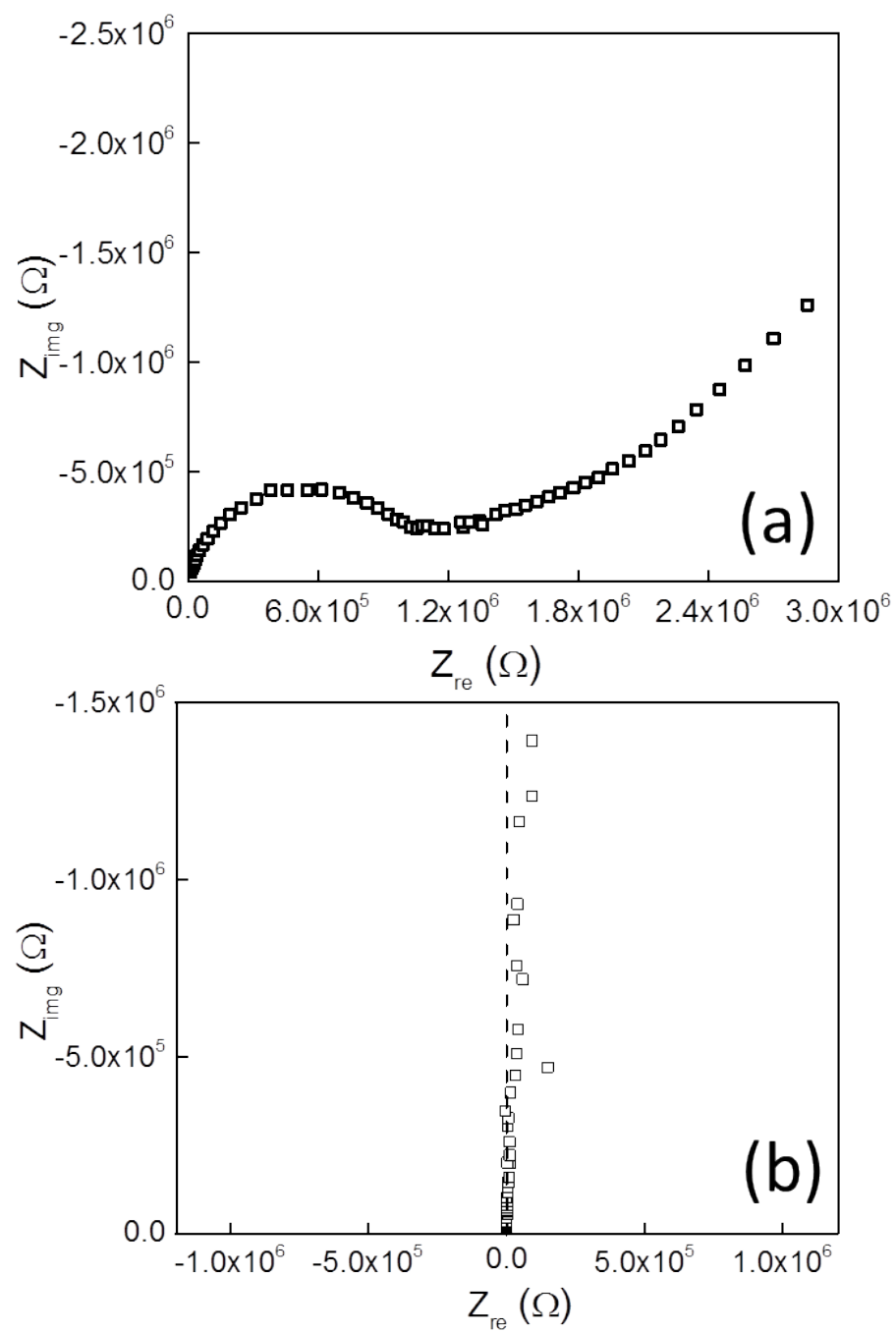


Figure S4. (a) Proton conductivity measured at 21 °C and 26% RH for the NdMo-MOF activated at 130 °C. (b) Proton conductivity measured at 21 °C under dry condition for the NdMo-MOF activated at 150 °C.

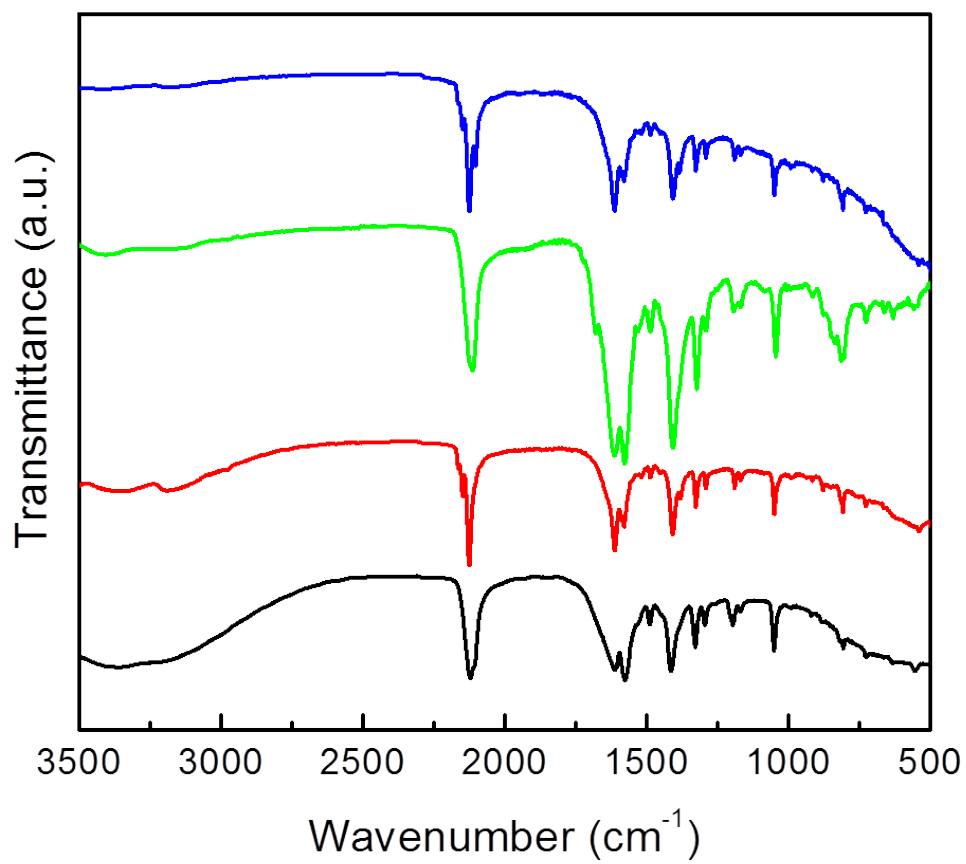


Figure S5. IR spectra of the as-synthesised NdMo-MOF (black), and the NdMo-MOF activated at 80 °C (red), 130 °C (green), and 150 °C (blue), respectively.

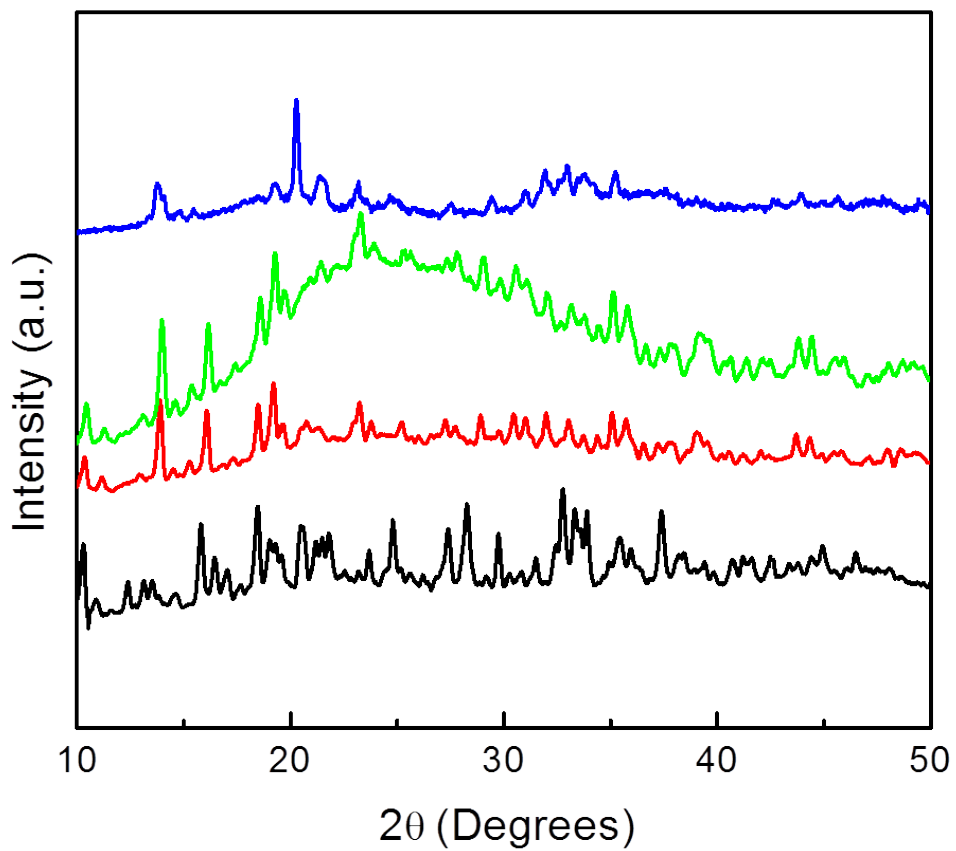


Figure S6. The PXRD pattern of the as-synthesised NdMo-MOF (black), and the NdMo-MOF activated at 80 °C (red), 130 °C (green), and 150 °C (blue), respectively.

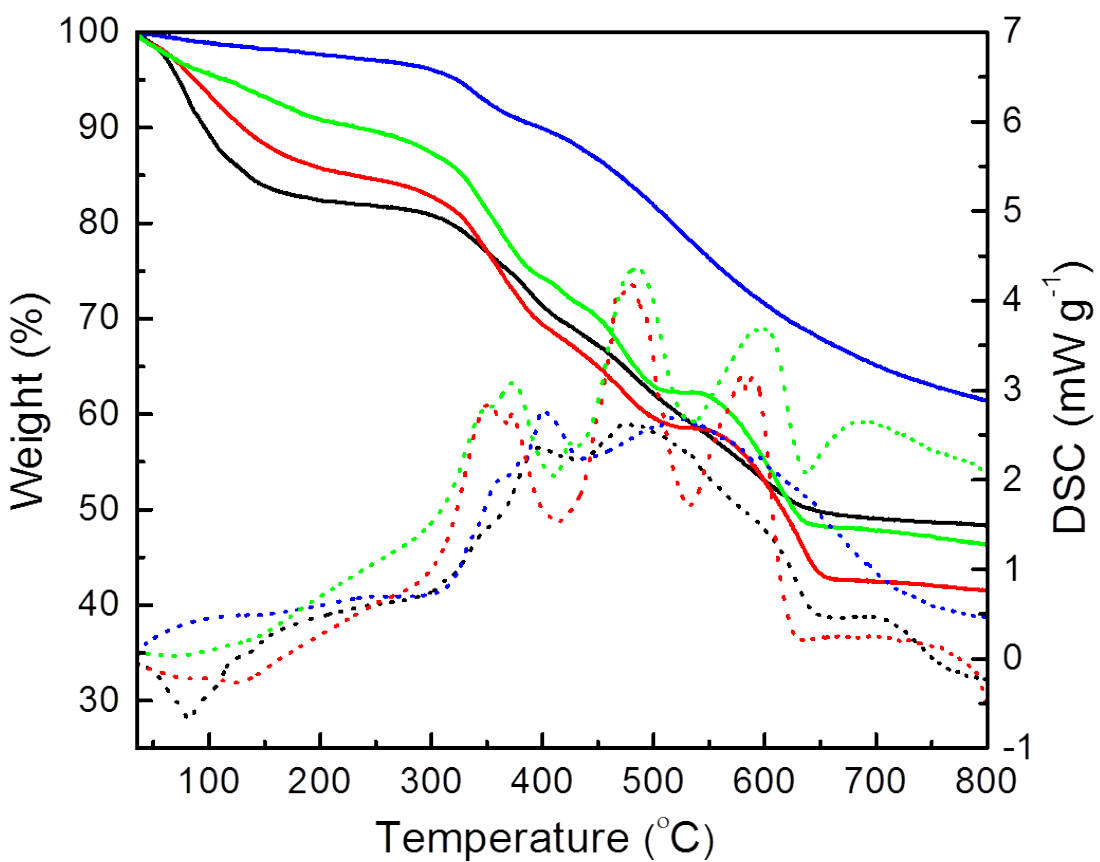


Figure S7. The TGA (continuous line) and DSC (dotted line) analyses for the as-synthesised NdMo-MOF (black), and the NdMo-MOF activated at 80 °C (red), 130 °C (green), and 150 °C (blue), respectively.

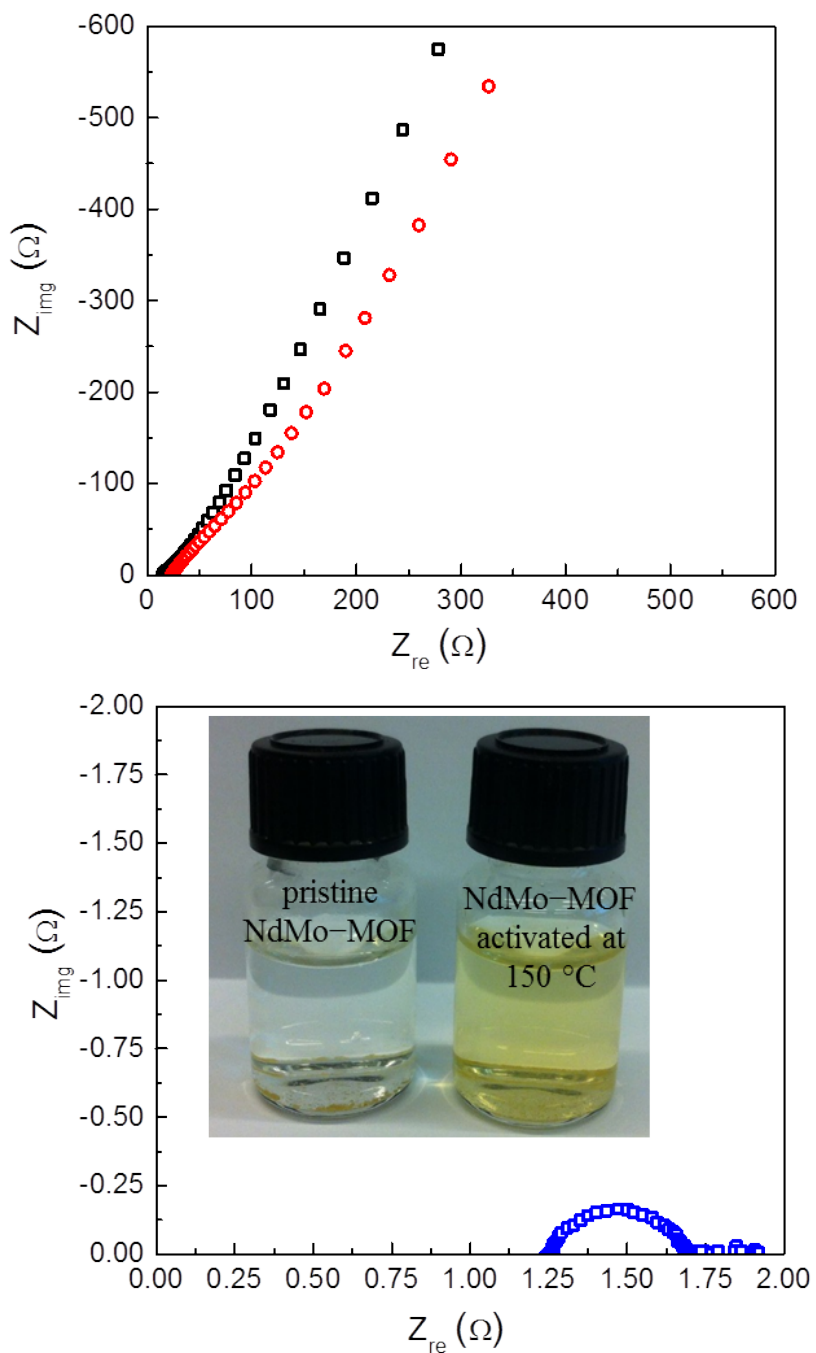


Figure S8. Nyquist plots measured at 21 °C and 98% RH for the NdMo-MOF activated at 80 °C (black), 130 °C (red) and 150 °C (blue) (top). The photo of the as-synthesised NdMo-MOF and the NdMo-MOF activated at 150 °C immersed in water (bottom).

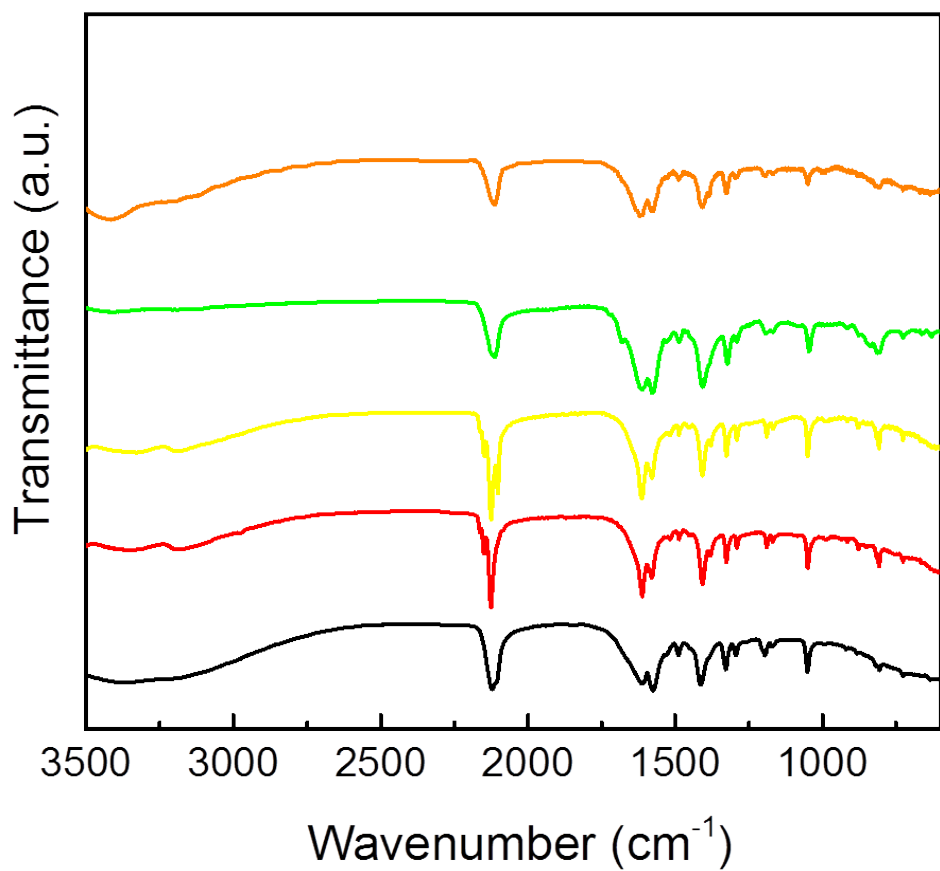


Figure S9. IR spectra of the as-synthesised NdMo-MOF (black), the NdMo-MOF activated at 80 °C (red) and after proton conductivity measurement (yellow), NdMo-MOF activated at 130 °C (green) and after proton conductivity measurement (orange), respectively.

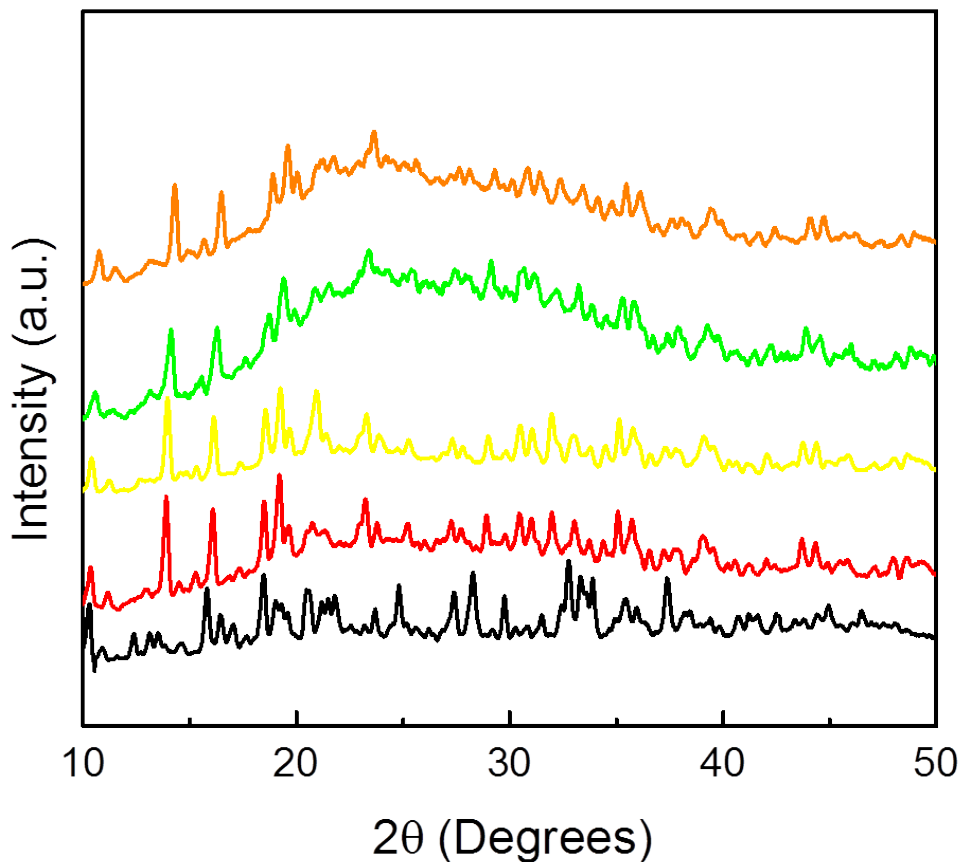


Figure S10. The PXRD patterns of the as-synthesised NdMo-MOF (black), the NdMo-MOF activated at 80 °C (red) and after proton conductivity measurement (yellow), NdMo-MOF activated at 130 °C (green) and after proton conductivity measurement (orange), respectively.

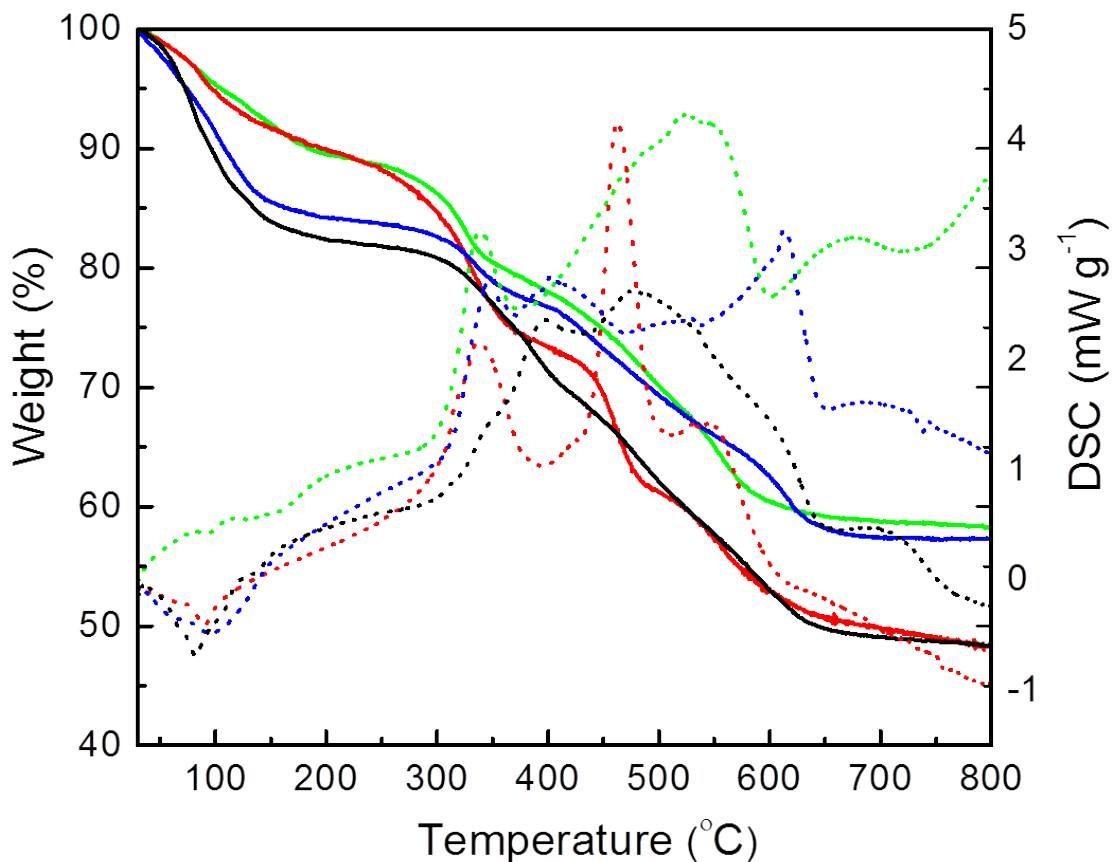


Figure S11. The TGA (continuous line) and DSC (dotted line) analyses of the as-synthesised NdMo-MOF (black) and for the NdMo-MOF activated at 130 °C and then immersed in water for 2 days (green), immersed in water for 1 week (blue) and after proton conductivity measurement (red).

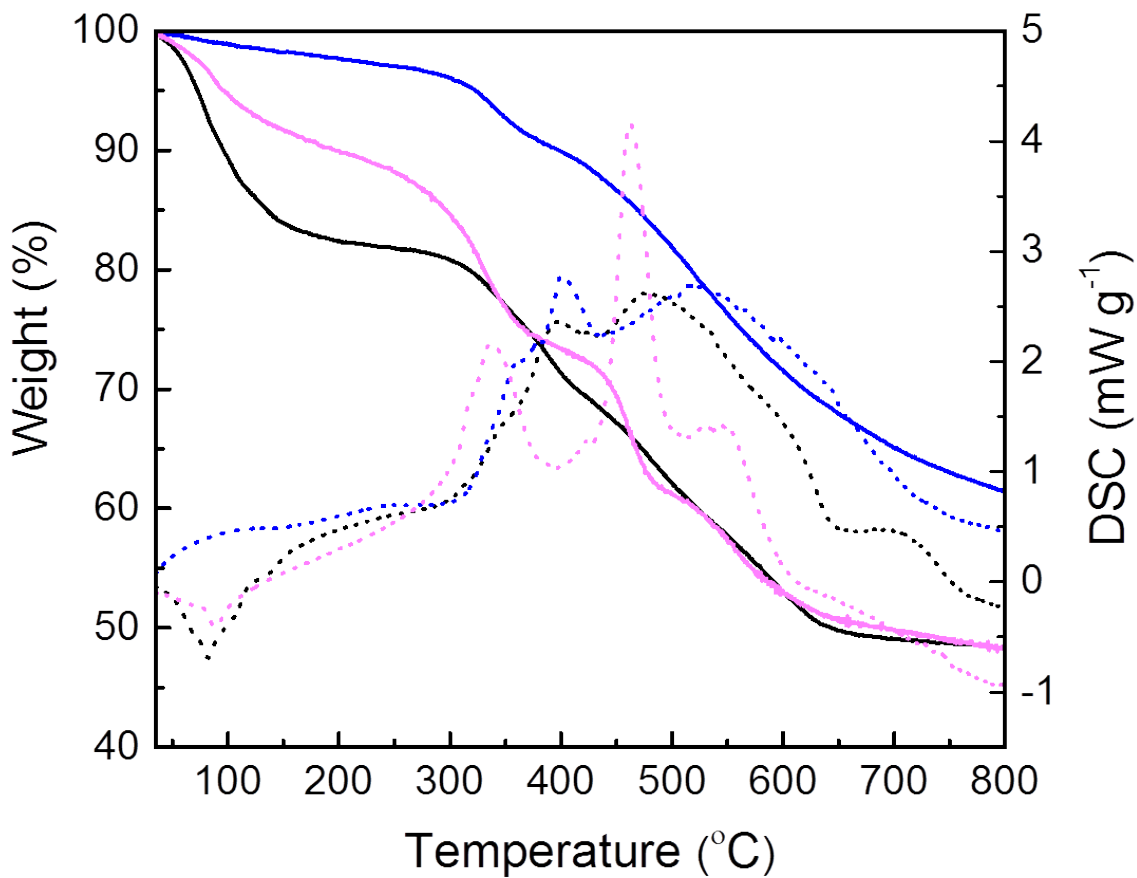


Figure S12. The TGA (continuous line) and DSC (dotted line) analyses of the as-synthesised NdMo-MOF (black) and for the NdMo-MOF activated at 150 °C (blue) and after water adsorption measurement (pink).

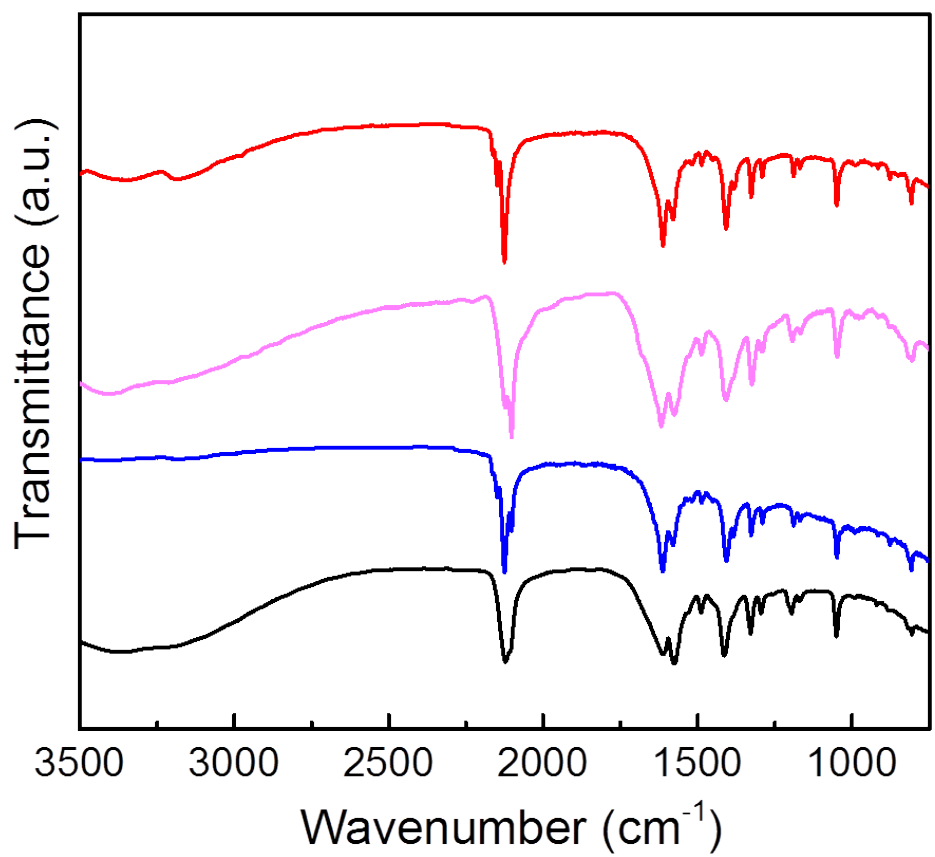


Figure S13. IR spectra of the as-synthesised NdMo-MOF (black), the NdMo-MOF activated at 150 °C (blue), after water adsorption measurement (pink) and after proton conductivity measurement (red), respectively.

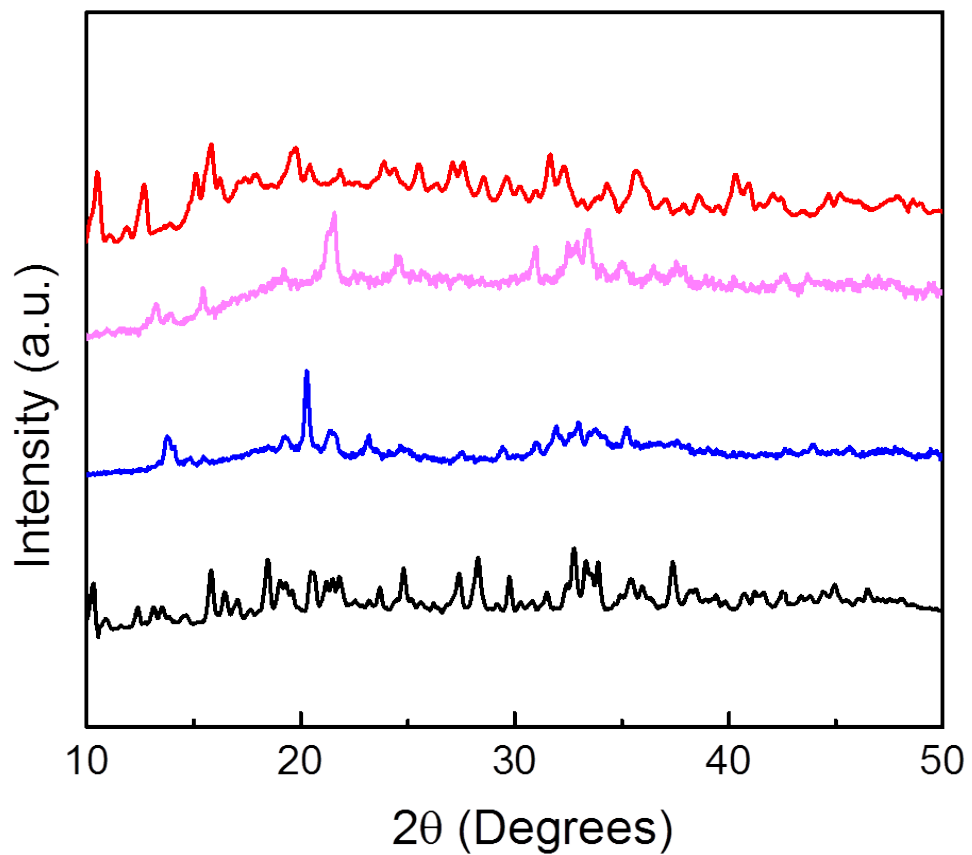


Figure S14. The PXRD patterns of the as-synthesised NdMo-MOF (black), the NdMo-MOF activated at 150 °C (blue), after water adsorption measurement (pink) and after proton conductivity measurement (red), respectively.

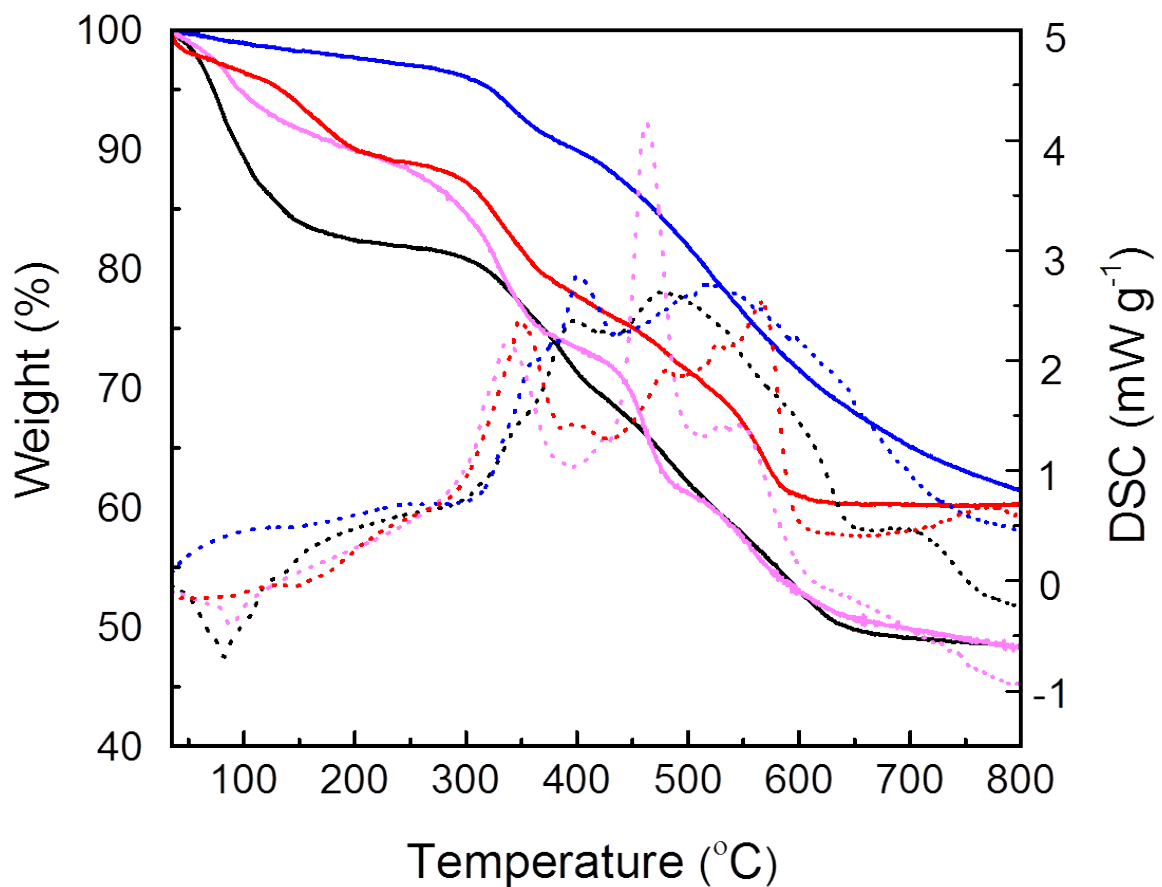


Figure S15. The TGA (continuous line) and DSC (dotted line) analyses of the as-synthesised NdMo-MOF (black), the NdMo-MOF activated at 150 $^{\circ}\text{C}$ (blue), after water adsorption measurement (pink) and after proton conductivity measurement (red), respectively.

Table S1. Performance indicators for water-mediated proton-conducting MOFs

Compound	Conductivity(S cm ⁻¹)	Activation energy (eV)	Measurement condition	Reference
[Mo ₅ P ₂ O ₂₃][Cu(phen)(H ₂ O)]·5 H ₂ O phen=phenanthroline	2.2×10 ⁻⁵	0.23	28 °C, 98 % RH	1
(NH ₄) ₂ (adp)[Zn ₂ (ox) ₃]·3 H ₂ O adp=adipate	8×10 ⁻³	0.63	25 °C, 98 % RH	2
V[Cr(CN) ₆] _{2/3} nH ₂ O	2.6×10 ⁻³	0.1	50 °C, 100 % RH	3
CMOF-3	3.5×10 ⁻⁵	0.17	RT, 98 % RH	4
HKUST-1-H ₂ O	1.5×10 ⁻⁵	n/a	RT, methanol vapor	5
[Zn(<i>I</i> -L _{Cl})(Cl)]·H ₂ O L _{Cl} =3-methyl-2-(pyridin-4-ylmethylamino)-butanoic acid	4.45×10 ⁻⁵	0.35	30 °C, 98 % RH	6
{H[Cu(Hbpdc)(H ₂ O) ₂] ₂ [PW ₁₂ O ₄₀]} _n H ₂ O, n = 7.5–8	1.56×10 ⁻³	1.02	100 °C, 98% RH	7
[EuL(H ₂ O) ₃]·2H ₂ O (L = N-phenyl-N'-phenylbicyclo[2.2.2]-oct-7-ene-2,3,5,6-tetracarboxdiimide tetracarboxylic acid)	1.6×10 ⁻⁵	0.91	75 °C, 97% RH	8
La(H ₅ DTMP)·7H ₂ O	8×10 ⁻³	0.25	24.1 °C, 98% RH	9
Eu ₂ (CO ₃)(ox) ₂ (H ₂ O) ₂]·4H ₂ O (ox = oxalate)	2.08×10 ⁻³	0.47 (25–90 °C) 0.26 eV (100–150 °C)	150 °C	10
[La ₃ L ₄ (H ₂ O) ₆]Cl·H ₂ O	1.7×10 ⁻⁴	0.7	110 °C, 98% RH	11
K ₂ (H ₂ adp)[Zn ₂ (ox) ₃]·3H ₂ O	1.2×10 ⁻⁴	0.45	98% RH	12
Eu-MOF	1.1 × 10 ⁻³	0.97	100 °C, 68% RH	13
[H(H ₂ O) ₂][Ca(HINO) ₄ (H ₂ O) ₅ (PW ₁₂ O ₄₀)	10 ⁻³	0.82	100 °C, 98% RH	14
[(Me ₂ NH ₂) ₃ (SO ₄)] ₂ [Zn ₂ (ox) ₃] _n	4.2×10 ⁻²	0.13	98% RH	15
JUC-125	1.5×10 ⁻⁴	0.32	50 °C, 97% RH	16
Cu ₃ [Co(CN) ₆] ₂ ·nH ₂ O	2.57×10 ⁻⁵	1.21	27 °C ,100 % RH	17
UiO-66	6.93×10 ⁻³	0.22	65 °C ,95 % RH	18
Na ₂ (OOCCH(OH)PO ₃ H)(H ₂ O) ₄	5.6 ×10 ⁻³	0.39	24 °C ,98 % RH	19

1. C. Dey, T. Kundu and R. Banerjee, *Chem. Commun.*, 2012, **48**, 266.
2. M. Sadakiyo, T. Yamada and H. Kitagawa, *J. Am. Chem. Soc.*, 2009, **131**, 9906.
3. S.-i. Ohkoshi, K. Nakagawa, K. Tomono, K. Imoto, Y. Tsunobuchi and H. Tokoro, *J. Am. Chem. Soc.*, 2010, **132**, 6620.
4. J. M. Taylor, R. K. Mah, I. L. Moudrakovski, C. I. Ratcliffe, R. Vaidhyanathan and G. K. Shimizu, *J. Am. Chem. Soc.*, 2010, **132**, 14055.
5. N. C. Jeong, B. Samanta, C. Y. Lee, O. K. Farha and J. T. Hupp, *J. Am. Chem. Soc.*, 2011, **134**, 51.
6. S. C. Sahoo, T. Kundu and R. Banerjee, *J. Am. Chem. Soc.*, 2011, **133**, 17950.
7. M. Wei, X. Wang and X. Duan, *Chem. Eur. J.*, 2013, **19**, 1607.
8. M. Zhu, Z.-M. Hao, X.-Z. Song, X. Meng, S.-N. Zhao, S.-Y. Song and H.-J. Zhang, *Chem. Commun.*, 2014, **50**, 1912.

9. R. M. Colodrero, P. Olivera-Pastor, E. R. Losilla, M. A. Aranda, L. Leon-Reina, M. Papadaki, A. C. McKinlay, R. E. Morris, K. D. Demadis and A. Cabeza, *Dalton Trans.*, 2012, **41**, 4045.
10. Q. Tang, Y. Liu, S. Liu, D. He, J. Miao, X. Wang, G. Yang, Z. Shi and Z. Zheng, *J. Am. Chem. Soc.*, 2014, **136**, 12444.
11. S. Begum, Z. Wang, A. Donnadio, F. Costantino, M. Casciola, R. Valiullin, C. Chmelik, M. Bertmer, J. Kärger and J. Haase, *Chem. Eur. J.*, 2014, **20**, 8862.
12. M. Sadakiyo, T. Yamada and H. Kitagawa, *J. Am. Chem. Soc.*, 2014, **136**, 13166.
13. R. Wang, X.-Y. Dong, H. Xu, R.-B. Pei, M.-L. Ma, S.-Q. Zang, H.-W. Hou and T. C. Mak, *Chem. Commun.*, 2014, **50**, 9153.
14. M. Wei, L. Chen and X. Duan, *J. Coord. Chem.*, 2014, **67**, 2809.
15. S. S. Nagarkar, S. M. Unni, A. Sharma, S. Kurungot and S. K. Ghosh, *Angew. Chem. Int. Ed.*, 2014, **53**, 2638.
16. X. Liang, F. Zhang, H. Zhao, W. Ye, L. Long and G. Zhu, *Chem. Commun.*, 2014, **50**, 6513.
17. C. Xiao, Z. Chu, X.-M. Ren, T.-Y. Chen and W. Jin, *Chem. Commun.*, 2015, **51**, 7947.
18. J. M. Taylor, S. Dekura, R. Ikeda and H. Kitagawa, *Chem. Mater.*, 2015, **27**, 2286.
19. M. Bazaga-García, M. Papadaki, R. M. Colodrero, P. Olivera-Pastor, E. R. Losilla, B. Nieto-Ortega, M. A. n. G. Aranda, D. Choquesillo-Lazarte, A. Cabeza and K. D. Demadis, *Chem. Mater.*, 2015, **27**, 424.